



Advancing Cancer Research: Intelligent Prediction and Analysis System Based on Deep Learning

¹Prathamesh S Birajdar, ²L.M.R.J. Lobo, ³Prajakta B Patil

¹Mtech student, ²Professor, ³Assitant Professor
¹CSE dept,

¹Walchand Institute of Technology, Solapur, India
²IT dept,

²Walchand Institute of Technology, Solapur, India
³ECE dept,

³Walchand Institute of Technology, Solapur, India

Abstract : Cancer screening is still a highly sensitive and divisive topic in the medical community. Numerous perspectives of view based on a little amount of reliable information are revealed by a study of publicly available data. Mammography screening age ranges and the value of the technique itself are still debatable topics. The value of lung or prostate cancer screening is still up for debate. The basis for recommendations and judgments for cancer screening should be trustworthy evidence, not good intentions, assumptions, or suppositions. In order to properly comprehend the current issues associated with testing for blood, prostate, and breast cancers, it is imperative to understand the underlying concepts and presumptions. This article will discuss the potential economical, legal, and radiation safety effects of whole-body CT or PET cancer screening. Images of the patient's body are captured during scanning. Abnormalities or cancerous tissues are now seen in the pictures using PET/CT. Localized areas of the body are affected by cancer. The stages of the cancer are then determined, and a classification of the type of cancer is created. The task of prediction is then automatically performed by a model that is constructed using machine learning algorithms. Thus, the entire procedure is automated.

IndexTerms - PET/CT scan, Convolutional Neural Network, Artificial Neural Network, Cancer Prediction, Deep Learning

I. INTRODUCTION

Medical imaging, which provides unique therapeutic and increasingly diagnostic capabilities that have an effect on patient care, is the cornerstone of modern healthcare. Although there are many different medical imaging modalities, they all deliver anatomical and useful facts about physiopathology and structure. The multi-modality 18F-Fluorodeoxy glucose (FDG) [1] positron emission tomography and computed tomography (PET-CT) [2] scanner is acknowledged as the tomography tool of special for the diagnosis, staging, and evaluation of therapeutic reply in several cancers. Areas of abnormal function can be found using PET-CT, which combines the anatomical localization provided by CT with the sensitivity of PET. While employing PET, healthier regions frequently absorb less FDG (a marker of glucose metabolism) than sick parts do. The geographic level of the sickness inside a specific structure, however cannot be consistently resolute due to the partial volume effect, tumor heterogeneity, and the intrinsically minor resolution of PET compared to CT and MRI [3] imaging. The anatomical localization of PET image interpretation locations with aberrant FDG uptake by CT improves the accuracy of image interpretation.

Kidney cells can change and proliferate out of control, becoming renal cortical tumors, the earliest indication of kidney cancer [4]. Benign, slow-growing, or malignant tumors are all possible. Because a malignant tumor is cancerous, it takes the ability to grow and blowout to additional portions of the body. While indolent tumors [5] can occasionally be cancerous. In his application, he will keep track of all the cancer-related illnesses as well as the body parts where they may be found. By comparing all of the information to prior research, he can also recommend ways to treat cancer so that patients can utilize the recommendations to manage their conditions.

To develop their system, he would follow the following steps:

1. Scanning the patient's body and keeping the pictures.
2. To find anomalies or cancerous tissues, use PET/CT.
3. Locate the area of the body that cancer has spread to.
4. Create a model using machine learning techniques to make predictions, classify cancer types.

II. RELATED WORK

This study includes prediction and classification of various cancers using images taken from a patient's body and analyzing the same. Matthias Baur and Felix Achilles [6] provide an innovative idea for crowdsourcing knowledge. Elsayed Amin Safaa

Mohammed Marey [7] present a YOLO-V4 built CAD system to pinpoint any alleged breast tumorous part and, if present, to accurately categories it as benign or malignant.

Alex Roshan Welikala and Paolo Remagnino [8] collected and annotated photos of the oral cavity in addition to presenting outcomes for automating oral cancer detection at an early stage. [9] In order to identify NSCLC in PET/CT images, this study provides a multi-modality attention-guided 3D identification outline. Liu Kanfeng and Ling Chen [10] lay the groundwork for multi-modality attention-guided 3D NSCLC finding in PET/CT pictures. TaeJin Ahn and Taewan Goo [11] remarked that the best DNN prototypical has an accuracy of 0.997 in the exercise customary and 0.979 in the exam customary, correctly differentiating between malignant and healthy data. Anish Simhal and Usama Chaudhary [12] described methods for retrieving color as well as texture data from VIA and VILI Cervigrammes via the processing of images. Saranya and Sasikala [13] show that patient data are amassed in large quantities in the medical field. Long Cheng and Yuzhen Niu [14] Used an artificial neural network and the H2O framework technique, they evaluated regular blood and blood chemistry information identified 33 relevant indices as GC biomarkers.

Hong-Jun Yoon and Shang Gao [15] offered a method for spreading DL NLP models among tumor databases while preserving patient privacy Zengyou Zhang And Bo Wang [16] showed how despite the fact that the Image Net-pre-trained model can be used for transfer knowledge, the technique of identifying the prostate MR image layer by layer falls under cross-domain learning because the model created on image.[17] This research offers our multimodality attention-guided 3-D detection method for NSCLC localization in PET/CT pictures. Azni Nasuha Ngisa [18] said in order to detect high-risk breast cancer patients. Thosini Mudiyansele, K. Bamunu [19] showed how in today's environment, accurate cancer detection is a significant issue. Formation of novel approaches for both the detection and prognosis of cancer could be implemented. Günay Melike Zeron Orman [20] showed results according to its accuracy findings, AIS can be regarded as a preferred method.

III. METHODOLOGY

He can use a methodology for the prediction of cancer-disease appearance based on the can be an incredibly beneficial tool to uncover hidden sights and prediction. Linear regression models [21] of machine learning technique are used for analyzing the current data with different linear regression models.

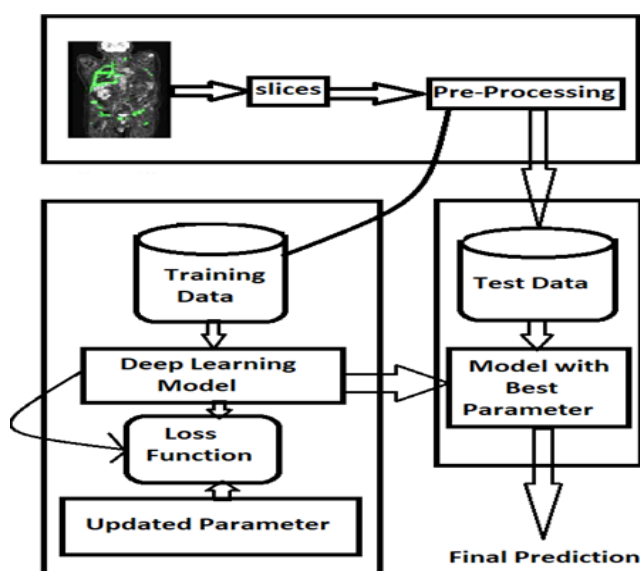


Fig 1 System overview

Artificial neural networks (ANNs) [22] They are recommended as an approach of using medical pictures to discover and define cancer, such as X-rays, CT scans, and MRI scans. This can be done using techniques such as object detection, semantic segmentation. [23] for categorizing spiteful and benevolent growths in mammograms.

A. Classification:

For assessing the performance of binary classification tasks including object identification, segmentation, and recognition, the F-measure [24] is a frequently used performance statistic. The F-measure, which combines accuracy and recollection, is used to assess a classifier's overall accuracy.

$$F\text{-measure} = 2 * (\text{accuracy} * \text{memory}) / (\text{accuracy} + \text{memory}) \dots (1)$$

The F-measure is particularly useful in image processing tasks, as it provides a balance between precision and recall. In object detection, for example, a high precision score is important to avoid false positives. Convolutional neural networks (CNNs) [25] is used for categorizing malignant and benign tumors in mammograms. Another example is using deep learning models for the recognition and separation of lung knobs in CT scans.

ANN are a powerful tool for detecting and localizing cancer in medical images. They can be trained to recognize specific features of cancer, and can provide accurate and automated predictions. However, the accuracy of these prediction scan varies depending on the quality and resolution of the images, as well as the specific architecture and training data used for the ANN. The Apriori method, which is the most widely used strategy for frequent pattern mining, was employed to minimize the processing cost. Another way that ANNs can be used to detect and localize cancer is by employing a process known as transfer learning. Handover knowledge is fine-tuning a pre-trained model for a particular task using a model that has already been taught, such as a CNN that has been trained on a big dataset. Since it enables the model to learn from a large dataset of photos and apply that information to a smaller dataset of medical images, this might be helpful in the context of medical imaging. This can help the model perform better and use less data and computer resources throughout the training process.

B. Segmentation:

Intersection over Union (IoU) [26] is a widely used performance metric in segmentation tasks to evaluate the accuracy of a model's predictions. The connection of the anticipated segmentation mask then the actual segmentation mask. The formula for calculating the IoU is:

$$\text{IoU} = \text{connection of predicted mask and ground truth mask} / \text{union of forecast mask and ground certainty mask} \dots (2)$$

To calculate the intersection and union of the two masks, we first need to convert the masks into binary arrays, where the background pixels are given a value of 0, the pixels corresponding to the object of interest are given a value of 1, and so on.

IV. EXPERIMENTAL SETUP AND RESULTS

The system is developed in Python using generic code to co-ordinate with the utilities of the system. The system will be supported with VRAM: 12GB NVIDIA RTX A6000, video card GeForce RTX 3080 and graphics card AMD Radon RX580. The data set required is downloaded from Kaggle.

The traditional F measure is designed as follows:

$$\text{F-Measure} = (2 * \text{Accuracy} * \text{Memory}) / (\text{Accuracy} + \text{Memory}) \dots (3)$$

It can first define the accurate positives (TP), wrong positives (FP), and wrong negatives (FN) as follows in order to simplify the equation:

The phrases for recollection and correctness are as follows:

$$\text{accuracy} = \text{TP} / (\text{TP} + \text{FP}) \dots (4)$$

$$\text{memory} = \text{TP} / (\text{TP} + \text{FN}) \dots (5)$$

Substituting these equations in the F-measure equation, we get:

$$\text{F-measure} = 2 * (\text{TP} / (\text{TP} + \text{FP}) * \text{TP} / (\text{TP} + \text{FN})) / (\text{TP} / (\text{TP} + \text{FP}) + \text{TP} / (\text{TP} + \text{FN})) \dots (6)$$

Simplifying this equation, we get:

$$\text{F-measure} = 2\text{TP} / (2\text{TP} + \text{FP} + \text{FN}) \dots (7)$$

It can calculate the accuracy as follows:

$$\text{Precision} = \text{Accurate Positives} / (\text{Accurate Positives} + \text{Wrong Positives})$$

$$\text{Precision} = 100 / (100 + 70)$$

$$\text{Precision} = 0.588$$

It can analyze the memory as follows:

$$\text{Recall} = \text{Accurate Positives} / (\text{Accurate Positives} + \text{Wrong Negatives})$$

$$\text{Recall} = 100 / (100 + 15)$$

$$\text{Recall} = 0.869$$

This shows that the model has poor precision, but excellent recall.

Finally, It can analyze the F-Measure as follows:

$$\text{F-Measure} = (2 * \text{Accuracy} * \text{Memory}) / (\text{Accuracy} + \text{Memory}) \dots (8)$$

$$\text{F-Measure} = (2 * 0.588 * 0.869) / (0.588 + 0.869)$$

$$\text{F-Measure} = (2 * 0.509) / 1.454$$

$$\text{F-Measure} = 1.018 / 1.454$$

$$\text{F-Measure} = 0.700$$

Cancer Types	Cancer Type Code	Precision	Recall	F-Score
Breast Cancer	1	0.588	0.869	0.700
Lung Cancer	2	0.6	0.833	0.696
Blood Cancer	3	0.562	0.9	0.690
Oral Cancer	4	0.555	0.862	0.674
Kidney Cancer	5	0.542	0.95	0.898

Table.1 F-Measure Accuracy table

It is a very logical metric to use connection over union. The overlap among the expected and ground truth annotations is separated by the combination of these to determine IoU.

$$J(A, B) = A \text{ Intersect } B / A \text{ Union } B \dots (a)$$

The Intersection over Union formula can be simply visualized; thus, it doesn't matter if you don't know the mathematical notation.

$$IoU = \text{Area of Overlap} / \text{Area of Union} \dots (b)$$

The Intersection over Union formula can be simply visualized; thus, it doesn't matter if you don't know the mathematical notation. It is evident that Model A's anticipated box joins with the Ground Truth more than Model B's does. The ground truth and Model C, however, overlap much more.

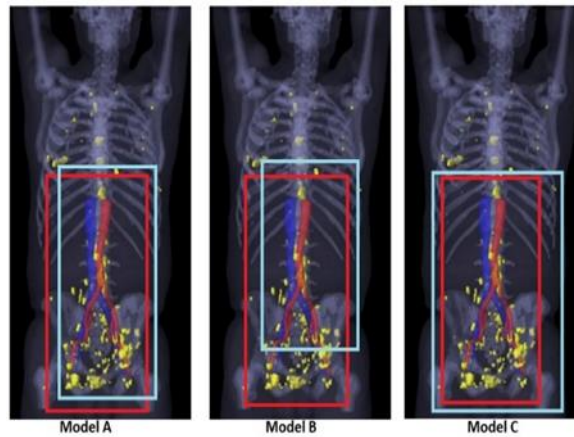


Fig2. Model indicating cancerous location

Yet it also overlaps with the background heavily. It is evident from models B and C that a score based just on overlap is unfair. True Positive: The region where segmentation mask and ground truth (GT) converge(S). This is logical AND operation.

$$TP = GT \cdot S \dots (i)$$

False Positive: The anticipated region away from the truth. The segmentation minus GT logical OR is represented by this.

$$FP = (GT + S) - GT \dots (ii)$$

False Negative: The quantity of pixels in the Ground Truth region that the model was unable to forecast.

$$FN = (GT + S) - S \dots (iii)$$

IoU, from Object Detection, it is the proportion of the intersected area to the sum of the prediction and ground truth areas

$$IoU = TP / (TP + FP + FN) \dots (iv)$$

Fig2 by using formula ...(iv) will obtain like this:

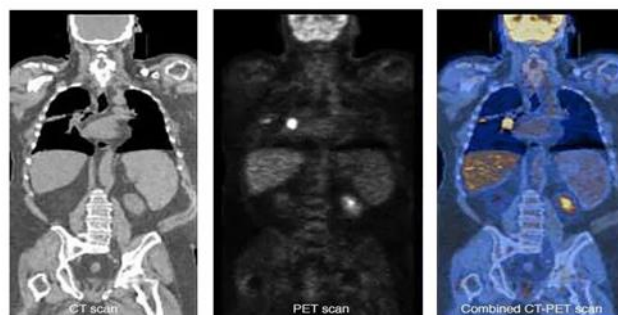


Fig3. Segmented Image

In the above session they have seen use of IOU formula for image segmentation and intersection to obtain the perfect effected area of image.

The accuracy of a machine learning model is calculated by comparing the predicted output of the model to the actual output for a set of labelled data.

$$\text{Accuracy} = (\text{Number of properly classified data points}) / (\text{Total number of data points}) \dots (vi)$$

For e.g. If there are 97 classified data points properly classified and 100 data points consider for the experimentation

$$\text{accuracy} = 97/100 = 0.97 \text{ or } 97\%$$

The throughput of a system refers to the rate at which it can process a certain amount of work over a given period of time.

$$\text{Processing time per image} = \text{Total processing time} / \text{Number of images processed}$$

For e.g., if the total time required for processing 200 images by a system is 10 min

$$\begin{aligned} \text{then Total processing time per image} &= 10 \text{ minutes} / 200 \text{ images} \\ &= 0.05 \text{ minutes per image} \end{aligned}$$

$$\text{Throughput} = 1 / \text{Processing time per image}$$

$$\begin{aligned} &= 1 / 0.05 \text{ minutes per image} \\ &= 20 \text{ images per minute} \end{aligned}$$

Comparison of Existing Systems Results with Implemented System Results				
Name of model	Accuracy Achieved by other authors	Accuracy by implemented system	Throughput Achieved by Other authors	Throughput by implemented system
CNN	95%	97%	10images/Min	20images/Min
ANN	87%	95%	5images/Min	10images/Min

Table .2

Here the system increases the accuracy and throughput. Table 2 is a comparison between results achieved by previous authors and expected improved accuracy and throughput.

V. CONCLUSION

In his study, CT and PET/CT scanners will be used for cancer detection, identification, and therapy monitoring. Depending on the visualized symptoms, the patient may choose to take precautionary steps. It is designed for the identification of many cancers, such as blood, breast, bladder, and kidney cancer. Detection, diagnosis, and treatment monitoring of cancer are all made possible by CT and PET/CT scanners. Patient and medical community awareness of cancer symptoms and use of CT are essential for early identification. Acid reflux can cause false alarms on PET/CT. The effectiveness of MUGA scans, chest X-rays, renal scans, and echocardiograms in assessing the ability of bodily organs to function while receiving chemotherapy and the potential for cancer spread in those organs. The utilization of automated information and gateways into clinic histories made obtainable to patients has enhanced clinic and patient access to automated information.

VI. ACKNOWLEDGMENT

Perhaps you want to take this opportunity to express our sincere gratitude to everyone who helped make our study endeavor on this topic a success. Throughout the research process, Prof. L.M.R.J. Lobo gave us tremendous advice, support, and encouragement, for which we are grateful. This deep learning and cancer research skills and expertise have been crucial in determining the focus and scope of our effort. Our team truly appreciates the patients and their family's willingness to grant us access to their medical records. The success of this study effort would not have been feasible without their collaboration and confidence. The results of our study, we hope, will increase cancer detection and therapy, ultimately enhancing the quality of life for individuals who are afflicted by this terrible disease.

REFERENCES

- [1] Hatt M, Visvikis D, Pradier O, Cheze-le Rest C. Baseline ¹⁸F FDG PET image-derived parameters for therapy response prediction in esophageal cancer. *Eur J Nucl Med Mol Imaging*. 2011 Sep;38(9):1595-606. doi: 10.1007/s00259-011-1834-9. Epub 2011 May 11. PMID: 21559979; PMCID: PMC3375481.
- [2] Awan MJ, Siddiqui F, Schwartz D, Yuan J, Machtay M, Yao M. Application of positron emission tomography/computed tomography in radiation treatment planning for head and neck cancers. *World J Radiol*. 2015 Nov 28;7(11):382-93. doi: 10.4329/wjr.v7.i11.382. PMID: 26644824; PMCID: PMC4663377.
- [3] G. Andria, A. M. L. Lanzolla, F. Attivissimo and T. Magli, "A new method to compare image quality in CT and MRI images," 2011 IEEE International Symposium on Medical Measurements and Applications, Bari, Italy, 2011, pp. 230-233, doi: 10.1109/MeMeA.2011.5966736.
- [4] N. Hadjiyski, "Kidney Cancer Staging: Deep Learning Neural Network Based Approach," 2020 International Conference on e-Health and Bioengineering (EHB), Iasi, Romania, 2020, pp. 1-4, doi: 10.1109/EHB50910.2020.9280188.
- [5] K. Hoyt, M. Mahoney and A. G. Sorace, "Four-dimensional molecular ultrasound imaging of tumor angiogenesis in a preclinical animal model of prostate cancer," 2014 IEEE International Ultrasonic Symposium, Chicago, IL, USA, 2014, pp. 1160-1163, doi: 10.1109/ULTSYM.2014.0285.
- [6] S. Albarqouni, C. Baur, F. Achilles, V. Belagiannis, S. Demirci and N. Navab, "AggNet: Deep Learning from Crowds for Mitosis Detection in Breast Cancer Histology Images," in *IEEE Transactions on Medical Imaging*, vol. 35, no. 5, pp. 1313-1321, May 2016, doi: 10.1109/TMI.2016.2528120.
- [7] G. Hamed, M. Marey, S. E. Amin and M. F. Tolba, "Automated Breast Cancer Detection and Classification in Full Field Digital Mammograms Using Two Full and Cropped Detection Paths Approach," in *IEEE Access*, vol. 9, pp. 116898-116913, 2021, doi: 10.1109/ACCESS.2021.3105924.
- [8] R. A. Welikala et al., "Automated Detection and Classification of Oral Lesions Using Deep Learning for Early Detection of Oral Cancer," in *IEEE Access*, vol. 8, pp. 132677-132693, 2020, doi: 10.1109/ACCESS.2020.3010180.
- [9] L. Chen et al., "Multimodality Attention-Guided 3-D Detection of Nonsmall Cell Lung Cancer in 18F-FDG PET/CT Images," in *IEEE Transactions on Radiation and Plasma Medical Sciences*, vol. 6, no. 4, pp. 421-432, April 2022, doi: 10.1109/TRPMS.2021.3072064.

- [10] K. -C. Chu, M. -Y. Xiao, C. -H. Chang, C. -H. Hsiao, Y. -C. Jiang and P. -Y. Tsai, "Preliminary Study of Relationship between Health Behavior and Breast Cancer," 2019 IEEE 20th International Conference on Information Reuse and Integration for Data Science (IRI), Los Angeles, CA, USA, 2019, pp. 410-413, doi: 10.1109/IRI.2019.00069.
- [11] T. Ahn et al., "Deep Learning-based Identification of Cancer or Normal Tissue using Gene Expression Data," 2018 IEEE International Conference on Bioinformatics and Biomedicine (BIBM), Madrid, Spain, 2018, pp. 1748-1752, doi: 10.1109/BIBM.2018.8621108.
- [12] M. N. Asiedu et al., "Development of Algorithms for Automated Detection of Cervical Pre-Cancers with a Low-Cost, Point-of-Care, Pocket Colposcope," in IEEE Transactions on Biomedical Engineering, vol. 66, no. 8, pp. 2306-2318, Aug. 2019, doi: 10.1109/TBME.2018.2887208.
- [13] S. Saranya and S. Sasikala, "Diagnosis Using Data Mining Algorithms for Malignant Breast Cancer Cell Detection," 2020 4th International Conference on Electronics, Communication and Aerospace Technology (ICECA), Coimbatore, India, 2020, pp. 1062-1067, doi: 10.1109/ICECA49313.2020.9297481.
- [14] B. Zhang et al., "Identification Tool for Gastric Cancer Based on Integration of 33 Clinical Available Blood Indices Through Deep Learning," in IEEE Access, vol. 10, pp. 106081-106092, 2022, doi: 10.1109/ACCESS.2022.3172477.
- [15] M. Alawad et al., "Privacy-Preserving Deep Learning NLP Models for Cancer Registries," in IEEE Transactions on Emerging Topics in Computing, vol. 9, no. 3, pp. 1219-1230, 1 July-Sept. 2021, doi: 10.1109/TETC.2020.2983404.
- [16] Y. Qian, Z. Zhang and B. Wang, "ProCDet: A New Method for Prostate Cancer Detection Based on MR Images," in IEEE Access, vol. 9, pp. 143495-143505, 2021, doi: 10.1109/ACCESS.2021.3114733.
- [17] L. Chen et al., "Multimodality Attention-Guided 3-D Detection of Nonsmall Cell Lung Cancer in 18F-FDG PET/CT Images," in IEEE Transactions on Radiation and Plasma Medical Sciences, vol. 6, no. 4, pp. 421-432, April 2022, doi: 10.1109/TRPMS.2021.3072064.
- [18] A.N. Ngisa and O. H. Fang, "Identifying High-Risk Breast Cancer Patients Using Microarray and Clinical Data," 2020 IEEE International Conference on Bioinformatics and Biomedicine (BIBM), Seoul, Korea (South), 2020, pp. 2040-2044, doi: 10.1109/BIBM49941.2020.9313175.
- [19] T. K. Bamunu Mudiyansele, X. Xiao, Y. Zhang and Y. Pan, "Deep Fuzzy Neural Networks for Biomarker Selection for Accurate Cancer Detection," in IEEE Transactions on Fuzzy Systems, vol. 28, no. 12, pp. 3219-3228, Dec. 2020, doi: 10.1109/TFUZZ.2019.2958295.
- [20] M. Günay, Z. Orman, T. Ensari, S. Oukid and N. Benblidia, "Diagnosis of Lung Cancer Using Artificial Immune System," 2019 Scientific Meeting on Electrical-Electronics & Biomedical Engineering and Computer Science (EBBT), Istanbul, Turkey, 2019, pp. 1-4, doi: 10.1109/EBBT.2019.8742075.
- [21] Prerita, N. Sindhvani, A. Rana and A. Chaudhary, "Breast Cancer Detection using Machine Learning Algorithms," 2021 9th International Conference on Reliability, Infocom Technologies and Optimization (Trends and Future Directions) (ICRITO), Noida, India, 2021, pp. 1-5, doi: 10.1109/ICRITO51393.2021.9596295.
- [22] M. C. Irmak, M. B. H. Taş, S. Turan and A. Haşiloğlu, "Comparative Breast Cancer Detection with Artificial Neural Networks and Machine Learning Methods," 2021 29th Signal Processing and Communications Applications Conference (SIU), Istanbul, Turkey, 2021, pp. 1-4, doi: 10.1109/SIU53274.2021.9477991.
- [23] K. V. Reddy and L. R. Parvathy, "An Innovative Analysis of predicting Melanoma Skin Cancer using Mobile Net and Convolutional Neural Network Algorithm," 2022 2nd International Conference on Technological Advancements in Computational Sciences (ICTACS), Tashkent, Uzbekistan, 2022, pp. 91-95, doi: 10.1109/ICTACS56270.2022.9988569.
- [24] Lavazza, L., Morasca, S. Comparing ϕ and the F-measure as performance metrics for software-related classifications. *Empire Software Eng.* 27, 185 (2022). <https://doi.org/10.1007/s10664-022-10199-2>
- [25] M. C. Younis, E. Keedwell and D. Savic, "An Investigation of Pixel-Based and Object-Based Image Classification in Remote Sensing," 2018 International Conference on Advanced Science and Engineering (ICOASE), Duhok, Iraq, 2018, pp. 449-454, doi: 10.1109/ICOASE.2018.8548845.
- [26] C. A. R. Goyzueta, J. E. C. De la Cruz and W. A. M. Machaca, "Integration of U-Net, ResU-Net and Deep Lab Architectures with Intersection Over Union metric for Cells Nuclei Image Segmentation," 2021 IEEE Engineering International Research Conference (EIRCON), Lima, Peru, 2021, pp. 1-4, doi: 10.1109/EIRCON52903.2021.9613150.